Journal of Materials Chemistry B

ROYAL SOCIETY OF CHEMISTRY

PAPER

View Article Online
View Journal | View Issue

Cite this: J. Mater. Chem. B, 2023, 11, 11357

Manipulation of cross-linking in PEDOT:PSS hydrogels for biointerfacing†

Anna P. Goestenkors, ‡[a] Tianran Liu, ‡[a] Somtochukwu S. Okafor, ‡[a] Barbara A. Semar,[b] Riley M. Alvarez,[a] Sandra K. Montgomery,[a] Lianna Friedman[a] and Alexandra L. Rutz *[a]

Conducting hydrogels can be used to fabricate bioelectronic devices that are soft for improved cell- and tissue-interfacing. Those based on conjugated polymers, such as poly(3,4-ethylene-dioxythiophene): polystyrene sulfonate (PEDOT:PSS), can be made simply with solution-based processing techniques, yet the influence of fabrication variables on final gel properties is not fully understood. In this study, we investigated if PEDOT:PSS cross-linking could be manipulated by changing the concentration of a gelling agent, ionic liquid, in the hydrogel precursor mixture. Rheology and gelation kinetics of precursor mixtures were investigated, and aqueous stability, swelling, conductivity, stiffness, and cytocompatibility of formed hydrogels were characterized. Increasing ionic liquid concentration was found to increase cross-linking as measured by decreased swelling, decreased non-network fraction, increased stiffness, and increased conductivity. Such manipulation of IL concentration thus afforded control of final gel properties and was utilized in further investigations of biointerfacing. When cross-linked sufficiently, PEDOT:PSS hydrogels were stable in sterile cell culture conditions for at least 28 days. Additionally, hydrogels supported a viable and proliferating population of human dermal fibroblasts for at least two weeks. Collectively, these characterizations of stability and cytocompatibility illustrate that these PEDOT:PSS hydrogels have significant promise for biointerfacing applications that require soft materials for direct interaction with cells.

Received 22nd June 2023,
Accepted 13th November 2023

DOI: 10.1039/d3tb01415k

rsc.li/materials-b

1. Introduction

Hydrogels are polymer networks with high water content (generally >70–99% water by mass[1]) and are used widely in biomedical applications for their similarities to native extracellular matrix.[2–4] In bioelectronics, there are many efforts to build devices based on these materials to achieve tissue-matching stiffness and other tissue-inspired properties.[5] For example, electrodes and other device components can be fabricated with hydrogels of conducting and semiconducting materials.[6,7] In general, there are two approaches to fabricating electronically conducting hydrogels: (1) adding conducting particles (*e.g.* carbon nanotubes, graphene, metal nanoparticles) beyond the percolation threshold or (2) polymerizing and/or cross-linking a conducting material into a polymeric network. These approaches often utilize a non-conducting polymeric network as the carrier hydrogel for particles or as an interpenetrating hydrogel network for improved mechanical properties and aqueous stability. Alternatively, methods of making conducting hydrogels comprised of solely conducting material ("pure" conducting hydrogels) are emerging. Investigations of these pure hydrogels may be easier to draw conclusions on properties intrinsic to conjugated polymers specifically (rather than other network components) towards contributing to our understanding of their hydrogel network properties and cell-material interactions.

Pure conducting material hydrogels have been made using conjugated polymers. Conjugated polymers have a bond structure of alternating double and single bonds and when doped, possess mobile charge carriers.[8] Furthermore, the organic nature of this semiconducting material enables tunable physicochemical properties and a variety of possible form factors. Common conjugated polymers for biointerfacing applications such as bioelectronics and tissue engineering include poly(3,4-ethylenedioxythiophene), poly(aniline), and poly(pyrrole).[8–10] Poly(3,4-ethylenedioxythiophene) polystyrene sulfonate (PEDOT:PSS) is commercially available as colloidal aqueous dispersions, facilitating its wide use. Additionally, PEDOT:PSS has a number of other desirable properties including excellent conductivity,

[a] Department of Biomedical Engineering, Washington University in St. Louis, 1 Brookings Dr, St. Louis, MO, USA. E-mail: rutzalexandral@wustl.edu
[b] Department of Mechanical Engineering and Materials Science, Washington University in St. Louis, 1 Brookings Dr, St. Louis, MO, USA

† Electronic supplementary information (ESI) available. See DOI: https://doi.org/10.1039/d3tb01415k

‡ Shared first authorship.

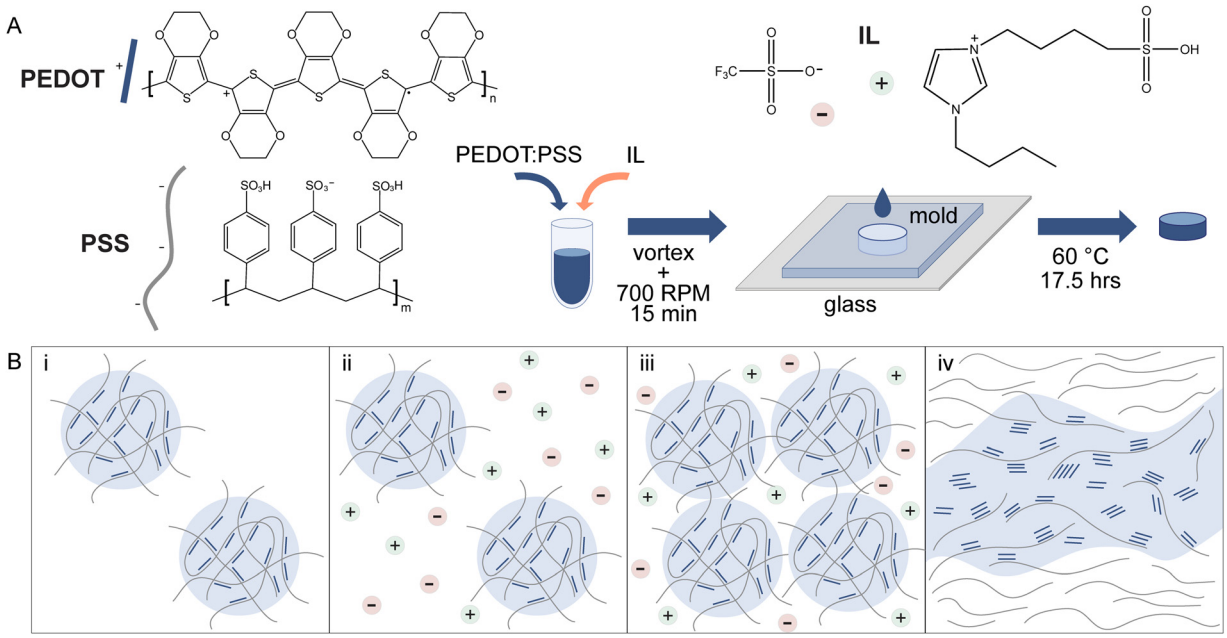

Fig. 1 Schematic of PEDOT:PSS-IL hydrogel fabrication and gelation mechanism. (A) Hydrogels were fabricated with mixing PEDOT:PSS colloidal dispersion and ionic liquid by first vortexing followed by stirring for 15 minutes. The mixture was pipetted into a silicone mold on glass and held at 60 °C for 17.5 hours for hydrogel formation. (B) Poly(3,4-ethylenedioxythiophene) (PEDOT, dark blue) is electrostatically bound to relatively higher molecular weight chains of polystyrene sulfonate (PSS, gray). In commercial colloidal aqueous dispersions, PEDOT:PSS exists as nano- to micro-sized, gel-like particles with a PEDOT-rich core (blue shaded region) and PSS-rich shell (i). An ionic liquid (IL), 4-(3-butyl-1-imidazolio)-1-butanesulfonic acid triflate, is added to weaken electrostatic interactions between PEDOT and PSS by performing charge screening (ii). Upon sufficient ionic strengths, PEDOT:PSS particles will aggregate and disassociated PEDOT is free to bind other PEDOT chains *via* pi–pi stacking (iii). The PEDOT-rich domains grow to form a physically cross-linked and interconnected network (iv), given sufficient fabrication and processing conditions.

aqueous stability when processed appropriately, cytocompatibility and emerging evidence of biocompatibility.[11] Within such aqueous dispersions, relatively low molecular weight PEDOT chains are bound to relatively high molecular weight PSS chains *via* electrostatic interactions. These ionic complexes exist as nano- to micro-sized,[12,13] gel-like particles in water with a PEDOT-rich core and PSS-rich shell (Fig. 1Bi).

Methods of making pure PEDOT:PSS hydrogels from these commercial aqueous dispersions have been described with various gelling agents: sulfuric acid,[14] 4-dodecylbenzenesulfonic acid[15] and ion pairs including ionic liquids[16–18] and metal cation salts (NaCl,[16] concentrated phosphate-buffered saline[19]). Additionally, processing steps such as annealing, solvent evaporation,[20,21] laser-induced phase separation[22] or solvent treatment[19] can be used alone or in combination with these gelling agents to fabricate PEDOT:PSS hydrogels. Ionic liquids, long used to improve the conductivity of PEDOT:PSS thin films,[23] have been shown to gel aqueous dispersions at sufficient ionic strengths and PEDOT:PSS concentrations.[16] When these liquid ion pairs are mixed with PEDOT:PSS dispersions, the anions and cations weaken the electrostatic interactions of PEDOT:PSS by performing charge screening of positively charged PEDOT and negatively charged PSS[16] (Fig. 1Bii). Particles aggregate and disassociated PEDOT is free to bind other PEDOT chains *via* π–π stacking (Fig. 1Biii). The PEDOT-rich domains grow to form a physically cross-linked and interconnected network, given sufficient conditions[24,25] (Fig. 1Biv).

Such methods of using gelling agents like ionic liquids are simple; the fabrication relies on mixing and casting, utilizes relatively mild conditions, and is substrate-independent. Ionic strengths to induce gelation from commercial aqueous

Alexandra L. Rutz

Alexandra Rutz graduated from University of Illinois in Urbana-Champaign (BS., 2011) where she double majored in Chemistry and Molecular and Cellular Biology. She obtained her PhD in Biomedical Engineering with a focus in Biomaterials from Northwestern University in 2016 (Chicago, IL, USA). As a Whitaker International Scholar and Marie Skłodowska-Curie Fellow, she conducted her postdoctoral research in the Malliaras Bioelectronics Lab at the University of Cambridge (UK). In 2021, Alexandra joined Washington University in St. Louis (MO, USA) as an Assistant Professor in the Department of Biomedical Engineering. Her lab is focused on bridging living systems with technologies through the design of materials and development of advanced manufacturing methods.

dispersions (1.0–1.3 wt% solids content) have been reported to range ~50–100 mM.[16] Weak gels result from mixing of PEDOT:PSS with ionic liquid after several days at room temperature[16] or 70 °C for 12 hours[17] (storage modulus G' ~ 1–100 Pa). Beyond stiffness, there have been few investigations of how ionic liquid concentration can be used to manipulate properties of pure PEDOT:PSS hydrogels. Tunable properties are attractive for applied research, and especially for biointerfacing, where being able to customize swelling properties, stiffness, and conductivity can allow for investigations of the impact of these parameters on biological outcomes and device performance.

In this study, we investigated if and how the concentration of ionic liquid impacts physical cross-linking of PEDOT:PSS hydrogels, since degree of cross-linking in turn impacts materials properties including swelling, stiffness, and conductivity.[26,27] We also investigated the potential of these pure conducting polymer hydrogels for biological interfacing. As part of this work, a critical degree of cross-linking was identified to eliminate significant disintegration in an aqueous environment. With this condition fulfilled, we then studied if these hydrogels can be used for mammalian cell culture and if such hydrogels could support a population of human primary cells through investigation of cell adhesion, morphology, viability, and proliferation over two weeks.

2. Experimental section

2.1. Preparation of PEDOT:PSS-ionic liquid hydrogel precursor mixtures

Colloidal aqueous dispersions of PEDOT:PSS (Clevios PH 1000) were acquired from Heraeus. PEDOT:PSS was filtered sequentially with 5 μm and 0.45 μm polytetrafluoroethylene (PTFE) syringe filters to remove large aggregates. According to supplier information, Clevios PH 1000 colloidal dispersions can range from 1.0–1.3 wt% and certificates of analysis of lots used in this study reported ~1.1–1.2 wt%. To prepare hydrogels of PEDOT:PSS, ionic liquid was used as a gelling agent (Fig. 1A). Hydrogel precursor mixtures were prepared by depositing neat ionic liquid (IL), 4-(3-butyl-1-imidazolio)-1-butanesulfonic acid triflate (Santa Cruz Biotechnology), in tared glass vials. PEDOT:PSS dispersions were utilized undiluted from stock (~12 mg mL^{-1}) or additionally, dilutions of PEDOT:PSS (~8–10 mg mL^{-1}) were prepared with deionized water prior to addition to ionic liquid. The appropriate amount of PEDOT:PSS dispersions was added to achieve ionic liquid concentrations ranging from 5–100 mg mL^{-1}. The vials were vortexed for one minute and then stirred for 15 minutes at 700 RPM. Unless otherwise stated, hydrogels were fabricated with undiluted PEDOT:PSS aqueous dispersions.

2.2. Determination of PEDOT:PSS-IL mixture phase, gelation kinetics, and viscosity

Initial screening of phase was conducted by preparing PEDOT:PSS-IL mixtures (2 mL) in glass vials (4.5 mL). The vial was sealed, stirred for 15 min, then immediately tilted and inverted to determine phase. Mixtures that fell to the bottom of the vial were categorized as liquids while mixtures that stayed at the top of the vial were categorized as gels.

The gelation kinetics and viscoelastic properties of PEDOT:PSS-IL mixtures were quantitatively characterized using a TA Instruments HR-20 rheometer. All measurements were taken with a cone-plate fixture (stainless steel plate of 40 mm diameter and 1.98889° cone geometry) and a solvent trap was used to prevent water evaporation. Viscosity of PEDOT:PSS-IL mixtures was investigated by performing rotational flow sweeps at shear rates of 1 1/s–100 1/s at 25 °C. To investigate gelation kinetics and viscoelastic properties, oscillatory time sweeps were run at 25 °C, 1% strain, and 1 rad s^{-1} angular frequency.

2.3. Preparation of PEDOT:PSS hydrogels

Silicone molds were prepared by punching 8 mm diameter cylinders (Sklar Tru-Punch Disposable Biopsy Punch) in sheets of cured elastomer, 5 mm thick. Briefly, the procedure consisted of mixing the elastomer and curing agent (Krayden Dow Sylgard 184 kit) at a 10 : 1 ratio (w : w) and degassing by centrifugation. The mixture was cast into polystyrene dishes and cured at room temperature overnight. Cut sheets were then adhered to glass slides with silicone sealant (Dow Corning 700 Industrial Grade) and were cured at room temperature for at least one hour prior to use.

A positive displacement pipette was used to deposit 250 μL of PEDOT:PSS-IL mixture (see 2.1) into silicone molds. A mold was placed in the bottom of a 35 mm polystyrene Petri dish inside of a secondary container (polypropylene jar, Nalgene®, 60 mL). Deionized water (2.7 mL) was added to the bottom of the secondary container around the outside of the Petri dish to maintain a local humidity during oven incubation. The containers were loosely capped and heated at 60 °C for 17.5 hours.

2.4. Hydrogel washing and swelling characteristics

PEDOT:PSS hydrogels were washed with deionized water using a wash volume of 50 times the precursor volume (12.5 mL). Water was exchanged at one and four hours after rehydration, then once daily thereafter. To measure hydrogel dimensions, images of the top (diameter, *XY*) and side (thickness, *Z*) were taken using a stereoscope (Nikon SMZ1270) and measurements were performed with NIS-Elements (Nikon). The hydrated mass of hydrogels was measured using an analytical balance after removing the hydrogel from water and removing excess water by dabbing the gel with a Kimwipe™. To determine the water mass and non-solvent mass within hydrogels, samples were removed at selected timepoints and placed in pre-weighed microcentrifuge tubes, frozen at −20 °C overnight, lyophilized, and weighed again.

2.5. Conductivity and mechanical characterization

The conductivity of PEDOT:PSS hydrogels was measured at room temperature using a four-point probe (Ossila, UK) with rounded tips for preventing damage to hydrogels. Excess water from hydrogels was removed by dabbing with Kimwipes™. Probes were positioned to be centered on the gel and the stage

supporting the hydrogel was slowly raised until all four probes had contacted the surface of the hydrogel. Following manufacturer recommendations, the stage was further raised to confirm sufficient contact between probes and hydrogel. Sheet resistance was measured and conductivity was calculated using the Van der Pauw equation. Conductivity values presented were taken from a mean of 50 conductivity recordings per measurement per sample, and the sample was measured three times to obtain a measurement average.

Compressive testing of hydrogels was performed using a TA Instruments ElectroForce 3200 System equipped with a 45 N load cell. The compressive strain rate was set at 1–2 mm min^{-1}, and samples were compressed to 1–2 mm displacement. Elastic modulus was determined by taking the slope of the stress–strain curve from 0% to 10% strain.

2.6. Assessment of PEDOT:PSS-IL hydrogel stability in cell culture conditions

Following swelling and washing, hydrogels were disinfected by incubating in 70% ethanol (10 mL) for 24 hours at room temperature. Hydrogels were then washed three times and incubated overnight in sterile 1X phosphate-buffered saline (PBS; Sigma Aldrich P3813) with 1% penicillin–streptomycin (Pen/Strep; 10 000 U mL^{-1} penicillin and 10 000 μg mL^{-1} streptomycin, Gibco 15140-122). Hydrogels were transferred to sterile well plates, UV disinfected for 2 hours in 1X PBS with 1% Pen/Strep, and stored at 4 °C until study. Hydrogels were always handled aseptically in a biosafety cabinet during preparation and for the duration of the study.

To begin *in vitro* assessment, hydrogels were each suspended in 3 mL of Dulbecco's Modified Eagle Medium (DMEM) (Corning) containing 10% fetal bovine serum (FBS) (Corning) and 1% Pen/Strep and placed in a cell culture incubator at 37 °C, 95% relatively humidity, and 5% CO_2. Exchanges of media were performed every seven days. Hydrogel swelling by dimensions, hydrated masses, and dry masses were characterized as described in 2.4.

2.7 Evaluation of cell attachment and expansion on PEDOT:PSS hydrogels

Normal adult human dermal fibroblasts (NHDF; Lonza CC-2511) were cultured according to supplier instructions. Briefly, fibroblasts were expanded in FGM™-2 Fibroblast Growth Medium-2 BulletKit™ (Lonza) on tissue culture flasks maintained at 37 °C in 5% CO_2. Hydrogels were transferred to sterile well plates coated with 2 wt% agarose (Sigma Aldrich) that presents a non-adhesive surface under the hydrogel. Hydrogels were then pre-conditioned for cell culture by incubating in the following media for 24 h at 37 °C: DMEM, 10% FBS in DMEM, or 100% FBS. Each media additionally contained 1% Pen/Step. Hydrogels were then washed in 1X PBS for 30 min to remove the pre-conditioning media, followed by replacement with cell culture media for at least 30 min prior to cell seeding.

Immediately before seeding, fresh culture media was added to sterilized and pre-conditioned hydrogels to barely submerge the top surface. Passage 5–6 NHDFs were seeded at 3500 cells cm^{-2}. The cell suspension was deposited drop-wise and evenly across the well, and the plate was gently shaken to further distribute the cells. To allow cells to settle, the well plate was left at room temperature for 30 min before transfer to a cell culture incubator. After overnight incubation, the culture media was replaced to remove unattached cells and was exchanged every other day thereafter.

To analyze cell attachment, cell-seeded hydrogels were first washed with DMEM followed by fluorescence staining at room temperature for 15 min. The staining solution contained 2 μM Calcein AM, 4 μM Ethidium homodimer-1 (EthD-1; LIVE/DEAD™, Invitrogen™), and 10 μg mL^{-1} Hoechst 33342 (BD) in DMEM. The samples were transferred to a glass bottom Petri dish (Thermo Scientific) and flipped so that the cell-seeded side was facing the microscope objectives. Epi-fluorescence imaging was performed with a Nikon Eclipse Ts2-FL inverted microscope. Three to four regions of interests (ROIs) were imaged per hydrogel to analyze most of the hydrogel surface. The acquired images were analyzed using NIS-Elements (Nikon) and the ROI measurements were averaged for each hydrogel.

2.8. Statistical analysis

For statistical analysis, ordinary one-way ANOVA with Tukey's or Dunnett's multiple comparison test and ordinary two-way ANOVA with Šídák's multiple comparison test were performed with GraphPad Prism. Results are presented as means with positive and negative standard deviation. Differences were categorized as statistically significant for $p < 0.05$.

3. Results and discussion

3.1. Concentration of ionic liquid in PEDOT:PSS dispersions affects gelation kinetics

Ionic liquids induce gelation by performing charge screening of PEDOT:PSS, helping to facilitate structural rearrangement of PEDOT and physical cross-linking including through π–π stacking (Fig. 1B). Hydrogels were prepared by stirring PEDOT:PSS dispersions and IL for 15 min at room temperature to fully mix components, followed by transfer to a mold and oven incubation at 60 °C for 17.5 hours (Fig. 1A). In this simple method of casting to define hydrogel shape, only a relatively short working time is needed to allow for mixture pipetting. However, more advanced forms of solution-based processing may require longer times and further may require a certain tolerance of solution properties. Here, we sought to measure PEDOT:PSS-IL mixture properties and gelation kinetics to inform potential compatibility with solution-based processing techniques and to access the working time of liquid mixtures at room temperature. Rheology was used to determine (1) if the mixtures are liquids or gels, (2) how long the mixtures are liquids (*i.e.* working time), and (3) what the viscosity is of all liquids and if this parameter changes over one hour.

In a qualitative assessment, we screened varying IL concentrations (0–100 mg mL^{-1}) in undiluted PEDOT:PSS dispersions (estimated 12 mg mL^{-1}). Immediately after 15 minutes stirring,

we evaluated the mixtures by tilting and inverting the vials (Fig. S1, ESI†). As the ionic liquid concentration increased, the viscosity appeared to increase as well (mixture showed greater resistance to flow). Tube inversion tests were conducted to qualitatively classify mixtures as liquids (falls to bottom of vial) or gels (stays at the top of the vial). Concentrations of IL using 40 mg mL^{-1} or less were qualitatively determined to be a liquid while 60 mg mL^{-1} or greater were qualitatively determined to be a gel. Similar trends were observed in diluted PEDOT:PSS dispersions (Fig. S1, ESI†).

Select formulations were then quantitatively assessed by oscillatory rheology to study the evolution of viscoelastic properties over about one hour at room temperature (Fig. 2, Tables S1 and S2, ESI†). PEDOT:PSS-IL mixtures were prepared in the same way as above (with 15 min stirring) prior to addition to the rheometer, and the time data was corrected to reflect the age of the mixture (time after IL addition). At an IL concentration of 10 mg mL^{-1} in PEDOT:PSS dispersions, the mixture was characterized as a liquid due to G'' (loss modulus) $\gg$ G' (storage modulus) and $\tan(\delta) > 1$ (δ – phase angle). Gelation was not observed over the studied period for this concentration. However, G' increased by about one order of magnitude and $\tan(\delta)$ decreased from 30.1 to 5.27, with both measures indicating cross-linking was occurring. At IL concentrations of 20, 30, and 40 mg mL^{-1}, the mixture was initially a liquid at the starting time of analysis, but gelation was observed within an hour as evidenced by the gel point (G'–G'' cross-over). At 60 mg mL^{-1}, the mixture was already a gel ($G' \gg G''$, $\tan(\delta) < 1$) at the starting time. Taken together, the rate of cross-linking increased with IL concentration as evidenced by a decreasing time for G'–G'' cross-over, ranging from not detected over 1 hour to less than 17 minutes (Table S1, ESI†). Mixtures that gelled had a G' of $\sim$1 Pa at the gel point but continued to cross-link further as evidenced by the increase in storage modulus over time ($G'_{75\ min}$ up to 83.3 Pa). It was expected that beyond the one hour investigated here that the gels continued to cross-link, and further, the mixtures were processed with oven incubation overnight (60 °C) rather than room temperature. Thus, the final modulus of these gels was determined by other means and is presented ahead in Section 3.4.

For all mixtures that were defined as liquids (10–40 mg mL^{-1} IL) when evaluated after stirring ($\sim$15–20 minutes), viscosity was measured by rotational rheology to analyze flow behavior and define values that may be compatible with certain processing techniques. All formulations were found to be shear-thinning (decreasing viscosity with increasing shear rates) (Fig. 3). As IL concentration increased, viscosity of the pre-gel mixture increased ranging from 0.03–0.11 Pa s (Table S1, ESI†). These viscosity values indicate that PEDOT:PSS-IL mixtures are anticipated to be compatible with solution-based processing techniques such as extrusion-based[18,28] and inkjet[29,30] printing and dip coating[31] which utilize solutions of viscosities that range from 0.1–1000 Pa s, 0.001 to 0.04 Pa s, and 0.05 to 0.5 Pa s respectively. However, the gelation kinetics of the mixture must be carefully considered. While 10 mg mL^{-1} IL is anticipated to have a working time of at least 80 min, there are increases in viscosity that may impact processing ($\sim$92% at shear rate of 100 1/s; Fig. S2 and Table S2, ESI†). Additionally, for mixtures containing 30 mg mL^{-1} IL or higher, processing times should ideally be limited to under 20 min. While this analysis was strictly done on mixtures defined as liquids, it should also be noted that mixtures of 60 mg mL^{-1} IL or greater were gels by 15 minutes yet were still able to be pipetted and spread to fill the silicone mold for hydrogel fabrication by casting.

3.2. Critical concentration of ionic liquid needed to form PEDOT:PSS hydrogels that remain integral upon aqueous swelling

Biointerfacing applications both *in vitro* and *in vivo* require operation in aqueous environments, whether that be cell culture media or biofluids (*e.g.* saliva, interstitial fluid, blood). Typically, hydrogels post-fabrication are in a relaxed state and will swell further when bathed in aqueous medium. For effective hydrogel fabrication, polymer cross-linking must occur at a sufficient degree. Otherwise, when exposed to water, substantial polymer may leave the hydrogel as non-network mass and

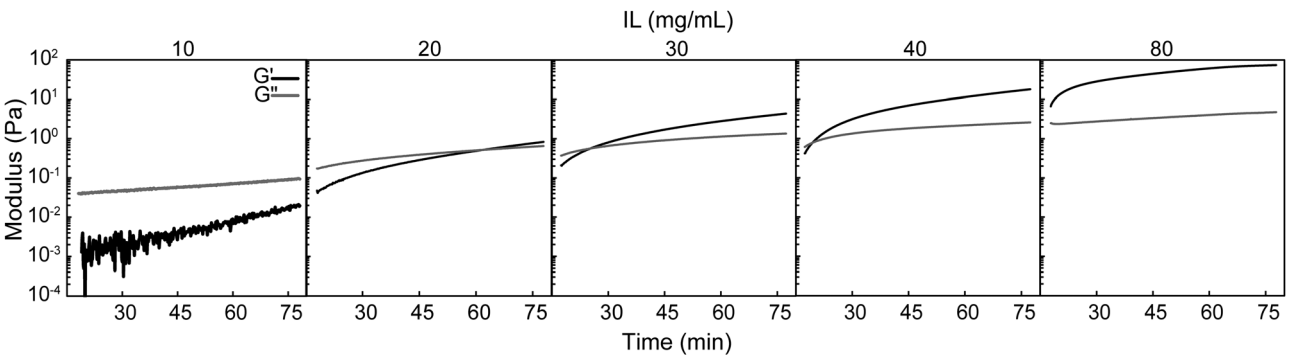

Fig. 2 Ionic liquid concentration affects gelation kinetics of PEDOT:PSS hydrogels. Oscillatory rheology over time to measure G' and G'', storage and loss modulus, respectively (representative plots). The transition from liquid to gel (G'–G'' cross-over), was captured for mixtures containing 20, 30, and 40 mg mL^{-1} IL over approximately 75 minutes. As the IL concentration increases, the time to G'–G'' cross-over shortened. At 10 mg mL^{-1} IL, the mixture remained a liquid over the time of study, while 80 mg mL^{-1} was already a gel. PEDOT:PSS-IL mixtures were stirred for 15 min prior to addition to the rheometer, and thus, the *x* axis represents time of mixture preparation (after IL addition).

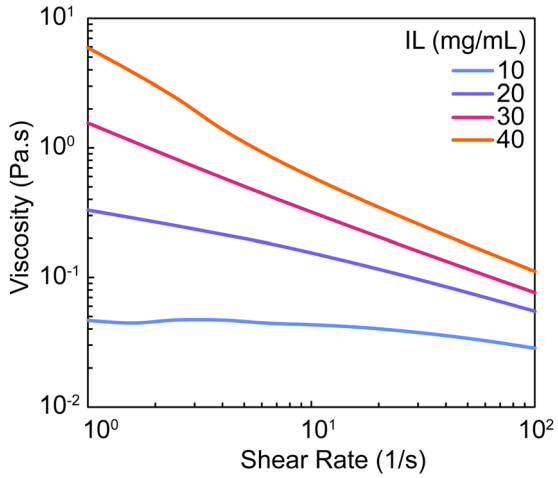

Fig. 3 Increasing ionic liquid concentration increases viscosity of liquid-phase PEDOT:PSS-IL mixtures. All liquid-phase hydrogel precursor mixtures are shear-thinning. Representative plots of viscosity as a function of shear rate measured 20 minutes after IL addition to PEDOT:PSS dispersion.

further, the polymer network may disintegrate upon swelling. To determine the critical cross-linking needed for hydrogel stability upon swelling, we screened varying IL concentrations (0–100 mg mL^{-1}) in undiluted PEDOT:PSS dispersion. This approach allowed us to quickly examine many formulations and identify candidates for further biointerfacing. After mixture preparation and oven incubation, all conditions appeared to result in a gel (Fig. 4A, top). Similar trends were observed in diluted PEDOT:PSS dispersions as well (Fig. S3 and S4, ESI†). As-fabricated gels had shrunk smaller than the mold at higher IL concentrations ($\geq$30 mg mL^{-1}) and as-fabricated diameters decreased with increasing IL concentration. While complete drying of the hydrogel was avoided by using a secondary container filled with water for local humidity during oven incubation, water evaporation was still observed with 58.3–74.2% loss of the precursor mixture starting mass (Fig. S5, ESI†).

The as-fabricated gels were then swollen in deionized water for 24 hours and hydrogel stability was qualitatively evaluated by visual inspection (Fig. 4A, bottom). The color of the wash water was noted for any obvious blue coloring which may indicate substantial non-network PEDOT:PSS. Hydrogel material in the water was examined if fully intact as a whole gel or if fragmented into pieces. At the specific oven conditions used, the critical IL concentration needed for hydrogel stability upon swelling was 20 mg mL^{-1} (Fig. 4B and Fig. S3 and S4, ESI†). In addition to gel fragmentation, substantial non-network PEDOT:PSS was only observed in formulations without IL, confirming its importance as a gelling agent. At IL concentrations of 5 and 10 mg mL^{-1}, the wash water appeared clear, yet the gel fragmented into pieces exceeding several millimeters while at IL concentrations of 20 mg mL^{-1} or more, PEDOT:PSS hydrogels remained as one whole piece.

Gels designated as stable at 24 hours displayed decreased swelling as the IL concentration increased, indicating that the resulting hydrogel networks became more densely cross-linked (Fig. 4A and C). The swollen diameters of hydrogels fabricated with 60, 80, and 100 mg mL^{-1} IL were not significantly different, and thus, these concentrations may not have resulted in substantially different networks. Across varying PEDOT:PSS concentrations, swollen gel diameters at 24 hours for a given IL concentration were similar (Fig. S6, ESI†).

To the best of our knowledge, only one previous study has been conducted on the effect of IL concentration on PEDOT:PSS phase. Leaf *et al.* analyzed PEDOT:PSS-IL mixtures after several days incubation at room temperature and reported critical IL concentration for gel formation ($\sim$50 mM or 20 mg mL^{-1} IL needed).[16] We obtained gels at lower ionic strength but we assume this is due to differences in processing time and temperature. Additionally, others have reported dimensional swelling of PEDOT:PSS hydrogels fabricated from IL but were only reported for a single IL concentration.[21,32] We contribute new findings of critical IL concentration for stability upon swelling, an important factor for use of hydrogels for biointerfacing, and the dependence of IL concentration on dimensional swelling (indicative of increased cross-linking).

3.3. PEDOT:PSS hydrogels reach equilibrium swelling within 48 hours and require washing to remove non-network mass

It is standard practice to wash hydrogels with copious amounts of water to remove all non-network components, including the base polymer as well as cross-linkers, gelling agents, or other molecules (Fig. 4A). Presence of such unbound components can impact assessments of cytocompatibility and biocompatibility, especially when cytotoxic reagents are used. In the case of PEDOT:PSS, the as-fabricated hydrogel is acidic due to presence of excess PSS and Brønsted acidic IL, and thus these hydrogels must be neutralized prior to biointerfacing. In addition to washing, immersing in water is also needed for hydrogels to reach an equilibrium swelling state when properties stabilize. Thus, since swelling can dramatically influence properties,[3,26] a fully swollen state should be achieved before testing for materials properties such as stiffness.

Hydrogels expected to have different degrees of cross-linking (IL concentrations 40 and 80 mg mL^{-1}) were incubated in deionized water for seven days with exchanges of the water being conducted as described in the methods (*i.e.* hydrogel washing). Swelling was measured by tracking hydrogel dimensions with time. Additionally, hydrogels were removed from the study at selected timepoints to measure its mass (*i.e.* hydrated mass) then frozen and lyophilized to obtain the dry mass (*i.e.* non-solvent mass). Using these values and the equations outlined in Fig. S7 (ESI†), water, network polymer, and non-network fractions were determined.

As observed by the consistent values of dimensions (Fig. 5B) and water mass (Fig. 5C left), hydrogels fabricated with 80 mg mL^{-1} IL mostly reached a fully swollen state one day after washing in deionized water. Hydrogels fabricated with 40 mg mL^{-1} IL continued to show slight changes in swelling by dimensions and water mass over 7 days (Fig. 5B and C). These changes mostly remained non-significant, with the exception of the *XY* dimension change between one and seven days

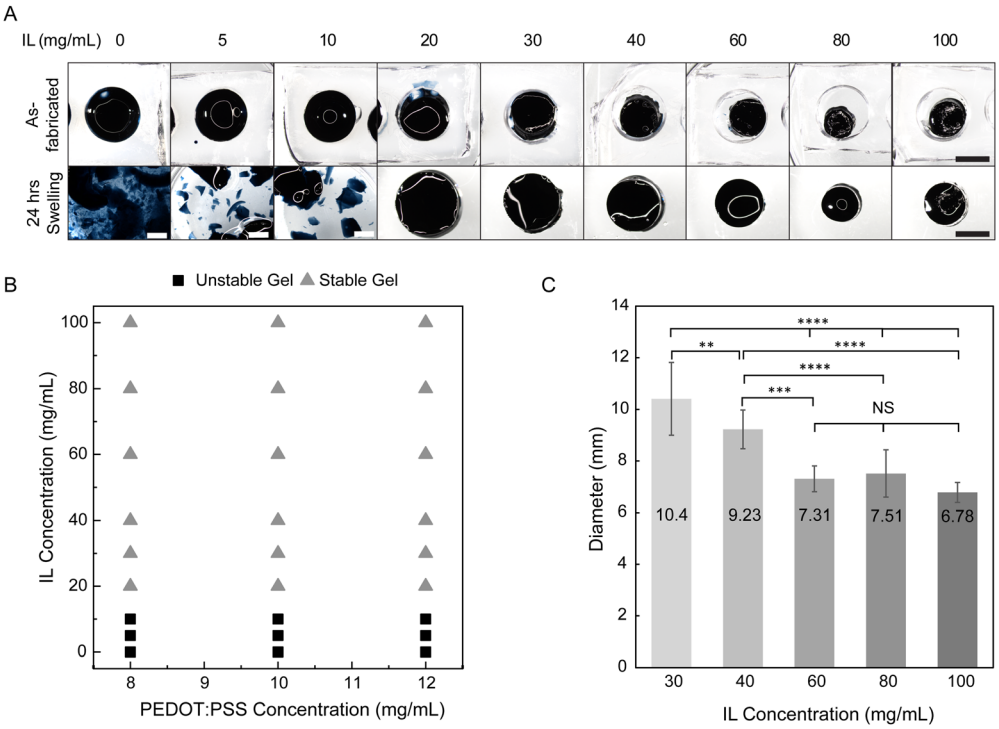

Fig. 4 Critical concentration of IL for PEDOT:PSS hydrogels that remain integral upon aqueous swelling (A) and (B) hydrogels were qualitatively evaluated for stability after 24 h of swelling in deionized water, images and scatter plot, respectively. Hydrogels fabricated from 10 mg mL^{-1} IL or less resulted in gels that fragmented and/or colored the wash water blue (designated unstable). Hydrogels fabricated from 20 mg mL^{-1} IL or above remained integral upon swelling. N = 2 per formulation. Representative images. All scale bars 5 mm; black scale bars apply to all images except those with a white scale bar. (C) As the IL concentration increased from 30 to 60 mg mL^{-1}, diameters of the resulting hydrogels significantly decreased. There were no significant changes in diameters among 60, 80, or 100 mg mL^{-1}. Mean and standard deviation presented. $N \geq 7$ per concentration. One-way analysis of variance (ANOVA) and Tukey's multiple comparison test. ****$P \leq 0.0001$ ***$P \leq 0.001$ **$P \leq 0.01$ *$P \leq 0.05$ non-significant (NS) $P > 0.05$.

(p = 0.0375). Interestingly, hydrogels fabricated with 80 mg mL^{-1} IL exhibited isotropic swelling (day 7 swelling XY/Z = 1.00 ± 0.05) while those with 40 mg mL^{-1} IL displayed slightly anisotropic swelling with larger swelling in the Z (day 7 swelling XY/Z = 0.87 ± 0.04) (Fig. 5B). Previously it has been demonstrated that cast and dry-annealed PEDOT:PSS generally exhibit anisotropic swelling in which volume increase is largely due to swelling of film thickness;[20,21] however, isotropic swelling has been reported in an equivalently formulated PEDOT:PSS droplet suspended to achieve equal dehydration in x, y, and z directions.[20] Since dimensional swelling of PEDOT:PSS hydrogels is highly dependent on the processing methods, the characterized differences between the as-fabricated and equilibrium swelling states can inform device or object design, especially for hydrogels with 3D microstructuring. For both formulations, we conclude swelling is largely complete with 48 hours.

To evaluate degree of cross-linking in hydrogels and removal of non-network components by washing, the lyophilized hydrogel mass was measured over seven days (Fig. 5C). The lyophilized hydrogel mass is referred to herein as the non-solvent mass (PEDOT:PSS and IL masses). Since IL is not anticipated to participate in the hydrogel network,[17,20] hydrogels were expected to substantially lose non-solvent mass after sufficient washing (76.9% and 87.0% expected for 40 and 80 mg mL^{-1} IL, respectively; dashed lines of Fig. 5C right). Within one day of washing, hydrogels had lost 79.1% and 89.5% of the initial non-solvent mass (40 and 80 mg mL^{-1} IL, respectively). Over seven days of washing, there was no additional detectable mass loss for hydrogels made from 80 mg mL^{-1}, whereas a non-significant decreasing trend was observed for those made from 40 mg mL^{-1} IL. The non-solvent mass changes were consistent with the observed trend in swelling by dimensions. Due to the fact that most mass loss was accomplished within two days washing, this wash protocol was used in all further experimentation.

After washing, the two hydrogel formulations had respectively lost 85.9% and 90.6% of their non-solvent mass, which corresponds to 8.97% and 3.65% beyond the expected mass loss due to IL removal (40 and 80 mg mL^{-1}, respectively; day 7, Fig. 5C right). This additional mass loss can be attributed to removal of excess PSS and PEDOT:PSS that is not linked to the network (Fig. 5A). The difference in non-solvent mass loss indicated that the IL concentration may be affecting the degree of PEDOT:PSS network cross-linking, resulting in different fractions of unbound polymer. To further investigate the effects of IL concentration on hydrogel network characteristics, additional groups of washed hydrogels (30–100 mg mL^{-1} IL) were measured for hydrated and non-solvent masses. Using these values, final water and polymer fractions were calculated, and additionally, mass loss was presented as the non-network

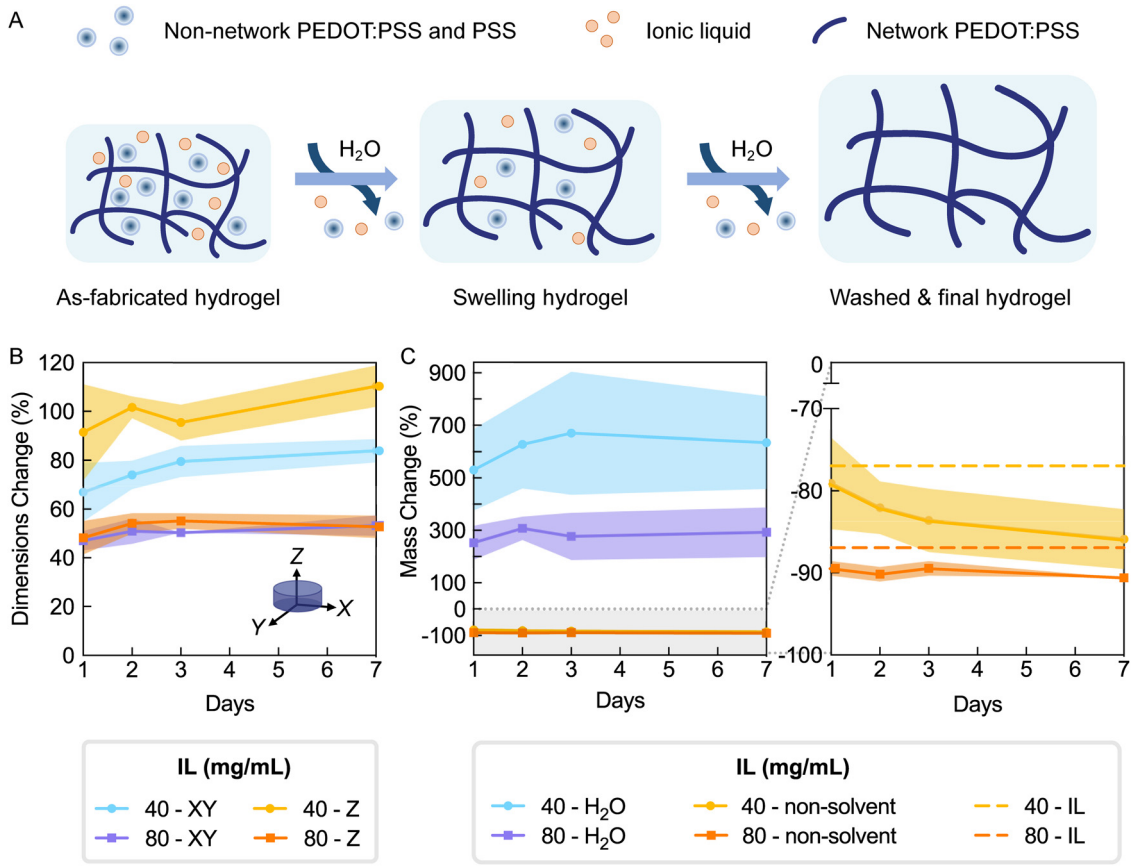

Fig. 5 PEDOT:PSS hydrogels reach equilibrium mass and dimensions after 24–48 h of swelling in deionized water. Hydrogels were fabricated with 40 and 80 mg mL^{-1} IL. (A) Schematic illustrating expected effects of water exchanges resulting in hydrogel swelling and non-network mass loss (IL, PSS, and non-network PEDOT:PSS). (B) Percent change in dimensions in *XY* and *Z* directions from as-fabricated measurements of each individual sample. There were no significant changes over time ($P > 0.05$), with the exception of days 1 to 7 for 40–*XY* ($P = 0.0375$). IL concentration significantly impacted dimensional swelling ($P < 0.0001$). (C) Percent change in water mass from as-fabricated average and percent change in non-solvent mass from calculated initial non-solvent mass (left). Plot on right is a zoomed in version of the gray shaded area showing percent change in non-solvent mass compared to the maximum theoretical mass loss due to IL (dashed lines). Differences among both water and non-solvent masses over time were not significant within a given IL concentration ($P > 0.05$). IL concentration significantly impacted changes in water and non-solvent mass ($P = 0.0009$ and $P = 0.0001$, respectively). Plot lines denote mean and colored shaded areas denote standard deviation. $N = 5–6$ per group per time point. Two-way analysis of variance (ANOVA) and Šidák's multiple comparison test.

fraction (Fig. S7, ESI†).[17,20] Equilibrium water fractions for all formulations were above 99% (Fig. S7B, ESI†), confirming the heavily hydrated state true of hydrogel materials. Furthermore, as the IL concentration for fabricating hydrogels increased from 30 to 100 mg mL^{-1}, the estimated polymer mass loss decreased from 15.2% to 3.1%, which corresponds to 53.3% to 28.9% of the initial PEDOT:PSS mass. This decreasing trend of non-network PEDOT:PSS further supported that increased IL concentration facilitated increased cross-linking of PEDOT:PSS. While these amounts may be high, mass loss due to PSS removal is expected. It has been previously reported that the PSS to PEDOT ratio in PEDOT:PSS films decreased from 2.1–2.5 to 1.3–1.6 after water exchange.[21,33]

3.4. Increasing ionic liquid concentration increases conductivity and stiffness of PEDOT:PSS hydrogels

After determining that the water exchanges over two days are sufficient to wash hydrogels for a stable mass and that hydrogels at this time appear to have reached equilibrium swelling, we investigated stiffness and conductivity of swollen hydrogels for various IL concentrations. Our swelling results (Sections 3.2 and 3.3) informed relationships between IL concentration and network properties, indicating cross-linking increased with increasing IL concentration. Stiffness and conductivity are both anticipated to increase with more cross-linking and thus are additional quantitative measures besides swelling that inform degree of cross-linking. Additionally, while IL is known to improve the conductivity of PEDOT:PSS thin films,[23] the impact of IL concentration on conductivity of PEDOT:PSS hydrogels has not been reported.

Stress–strain curves of hydrogels were generated by compression testing. As IL concentration increased, the ultimate strength significantly increased from 0.11 ± 0.055 to 0.79 ± 0.49 kPa for IL concentrations 30 to 100 mg mL^{-1} (p-value = 0.0007) (Fig. 6A and Table S3, ESI†). Generally, the elastic modulus increased with ionic liquid concentrations; although,

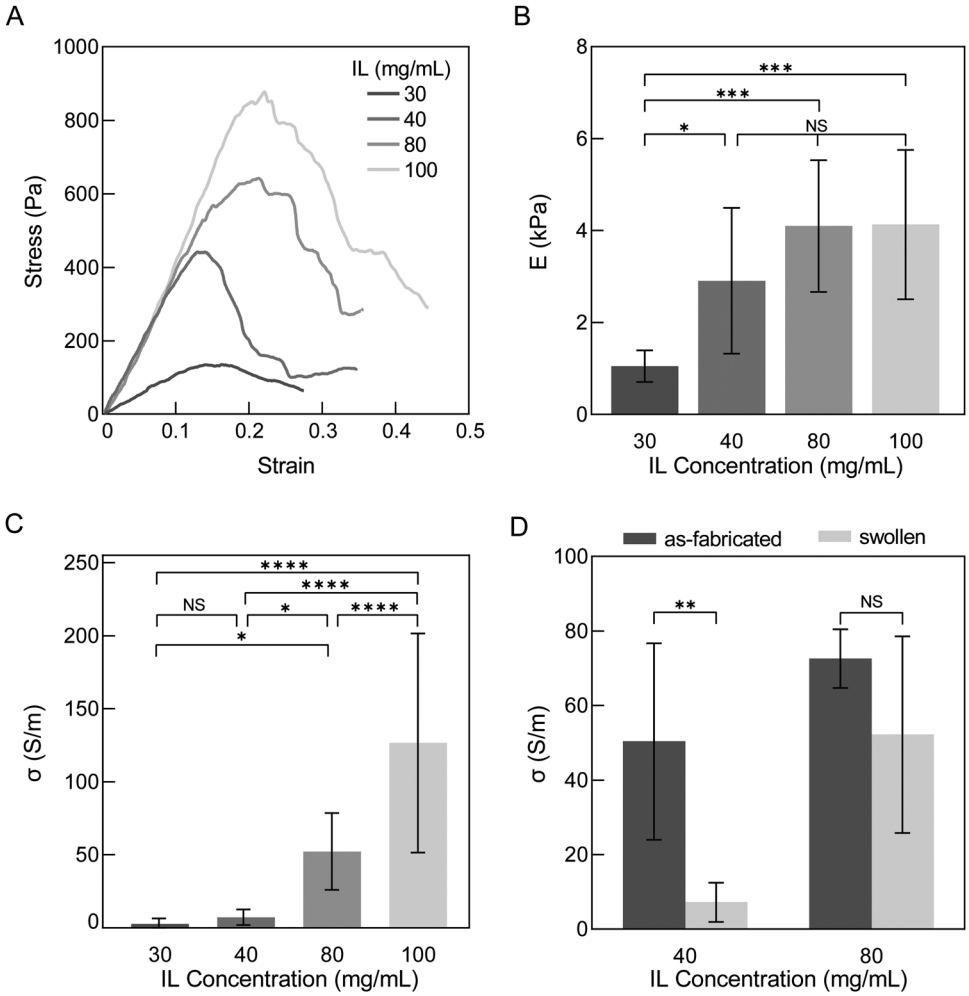

Fig. 6 Ionic liquid concentration increases stiffness and conductivity of swollen and washed PEDOT:PSS hydrogels. (A) Representative stress–strain curves of hydrogels of various IL concentrations in compression (moving average of 100). (B) Compressive elastic modulus increases with IL concentration. (C) Conductivity increases with IL concentration. (D) Conductivity of hydrogels decreases from as-fabricated to swollen and washed state. Mean and standard deviation presented. $N \geq 7$ for (A) to (C), $N \geq 3$ for D. One-way analysis of variance (ANOVA) and Tukey's multiple comparison test for (B) and (C). Two-way analysis of variance (ANOVA) and Šídák's multiple comparison test for (D). ****$P \leq 0.0001$ ***$P \leq 0.001$ **$P \leq 0.01$ *$P \leq 0.05$ non-significant (NS) $P > 0.05$.

only significant increases were observed from 30 to 40 mg mL^{-1}, 30 to 80 mg mL^{-1} and 30 to 100 mg mL^{-1} IL (1.05 to 2.91, 4.10 and 4.13 kPa, p-value = 0.0498, 0.0004 and 0.0003, respectively; Fig. 6B). The magnitude of these mean modulus values from all groups confirm further cross-linking over time beyond the first 75 minutes after IL addition studied by rheology (Section 3.1). Overall, the PEDOT:PSS hydrogels were still exceedingly soft for a conducting material[34] and have an elastic modulus ideal for interfacing with cells and soft tissues, which generally have moduli ranging from 0.5–10 kPa.[35]

Conductivity of hydrogels displayed a wider range of values than elastic modulus and increased with increasing IL concentration (2.75 ± 3.75 to 127 ± 75.1 S m^{-1} for 30 and 100 mg mL^{-1}, respectively; p-value <0.0001; Fig. 6C). This trend is similar to that reported of PEDOT:PSS thin films where ionic liquid is used as an additive to increase conductivity.[36] The conductivity values of these conducting hydrogels are comparable to other reports of pure PEDOT:PSS hydrogels made with mixing and casting techniques (10–20 S m^{-1}).[15,17,37] With more extensive preparation and/or post-fabrication processing steps such as annealing, acid or solvent treatment, conductivity and modulus of PEDOT:PSS hydrogels have been reported to be 2–3 orders magnitude higher than the hydrogels here ($\sim$2 MPa and $\sim$4000 S m^{-1}),[20,38,39] and additionally, display lower water fractions ($\sim$70–89%).[20,21,40] With even more extensive processing, PEDOT:PSS thin films have conductivity and modulus values higher than post-fabrication processed hydrogels (>100 MPa and up to 400 000 S m^{-1}) and are expected to have even lower water fractions (<50%).[20,23] We thus observe from the literature a spectrum of PEDOT:PSS properties dependent on processing. While no explicit definition exists for classifying materials as hydrogels by its water fraction, it should be noted that lower water and higher polymer fractions result in higher stiffness (100 s kPa to MPa), which may go beyond the desired tissue-mimicking softness. Thus, processing and the

balance of competing properties should be carefully considered per application. Our results here indicate that at high ionic liquid concentrations in PEDOT:PSS, hydrogels can have moderate conductivities ($\sim$125 S m^{-1}) while maintaining soft tissue-matching stiffness and a highly hydrated environment (>99% water by mass), both ideal for biointerfacing.

To illustrate the importance of evaluating conducting hydrogel properties in a fully swollen and washed state, we compared the mean conductivities of as-fabricated and washed PEDOT:PSS hydrogels between a less cross-linked and more cross-linked group (40 and 80 mg mL^{-1} IL concentration, respectively) (Fig. 6D). Mean conductivities decreased from this as-fabricated, relaxed state to the washed, swollen state, but the difference between these states was only significant for 40 mg mL^{-1} (p-values = 0.0020 and 0.1219 for 40 and 80 mg mL^{-1} IL, respectively). The change in conductivity between as-fabricated to swollen states was observed to be a 85.7% and 28.1% decrease in mean for 40 and 80 mg mL^{-1} IL, respectively. As previously discussed, washing is needed to remove IL and excess PSS. PSS is insulating and its removal has been reported to result in an increase in conductivity in PEDOT:PSS thin films.[41] Instead, here, conductivity decreased after washing. We believe the decrease in conductivity from as-fabricated to swollen states in hydrogels could be due to two reasons: (1) significant swelling that furthers distance between PEDOT-rich domains and/or (2) loss of PEDOT:PSS with washing as part of the non-network fraction. Our results are in agreement with this hypothesis as gels of 80 mg mL^{-1} IL resulted in less *XY* dimensional swelling (84.0% and 53.3% for 40 and 80 mg mL^{-1}, respectively) and less estimated PEDOT:PSS loss than 40 mg mL^{-1} IL (39.2% and 32.6% for 40 and 80 mg mL^{-1}, respectively; Fig. 5). Additionally, our results are consistent with Liu *et al.* who reported that the conductivity of PEDOT:PSS hydrogels decreased when swollen[42] and with Leaf *et al.* who reported that when water was evaporated from hydrated PEDOT:PSS hydrogels conductivity significantly increased from 1.2 to 5000 S m^{-1}.[16]

In summary, swelling (Fig. 4C and 5), mechanical properties, and conductivity collectively indicate that higher IL concentrations induce more cross-linking. Most of the observed significant differences, however, were between hydrogels of 30 or 40 mg mL^{-1} (less cross-linked) with those of 80 or 100 mg mL^{-1} (more cross-linked), and little differences in-between. Based on these results, we down-selected to investigating only hydrogels of 40 and 80 mg mL^{-1} IL to compare less and more cross-linked networks when evaluating their potential for biointerfacing applications.

3.5. PEDOT:PSS hydrogels are stable in cell culture conditions for at least 28 days when cross-linked sufficiently

Many *in vitro* biointerfacing applications of hydrogel-based bioelectronics will require continuous operation and stable properties in a cell culture environment. In these instances, conducting hydrogels must not significantly degrade over the use life-time since degradation will result in decreased cross-linking, increased swelling and decreased stiffness, which in turn impacts cell motility and spreading.[3,27] Therefore, sufficient cross-linking is needed to prevent degradation and maintain hydrogel integrity to give rise to consistent swelling and stiffness throughout the culture period. To the best of our knowledge, no study has been conducted on the stability of pure PEDOT:PSS hydrogels in sterile cell culture conditions. We analyzed stability of PEDOT:PSS hydrogels over 28 days by measuring hydrated mass and dimensional swelling (percent change in diameter) previously utilized in hydrogel studies to quantify degradation.[43,44] As a hydrogel degrades, water is able to more greatly permeate the hydrogel causing increases in hydrated mass and hydrogel dimensions.[27]

Disinfected PEDOT:PSS hydrogels made with two IL concentrations (40 and 80 mg mL^{-1}) were suspended in Dulbecco's Modified Eagle Medium (DMEM) containing 10% fetal bovine serum (FBS) and 1% Pen/Strep. Hydrogels were held within a cell incubator over the study period (5% CO_2, 95% relative humidity, 37 °C). Notably, the hydrogels had undergone washing as defined by our studies in Section 3.3 prior to the start of the study to ensure hydrogels were in a stable state prior to investigation. Over the study period, PEDOT:PSS hydrogels showed no visible fragmentation or break-down (Fig. 7A). As well, during the manual handling required for measurements, no apparent differences in hydrogel robustness or handleability were observed throughout the study. For quantified measures, there were no significant changes in diameters or hydrated masses over the study period (Fig. 7B and C). Collectively, these measures indicate that the PEDOT:PSS hydrogels did not undergo significant degradation over 28 days.

Additionally, we measured the dry mass of the hydrogels to remove mass contributions from water to better focus on non-solvent mass over time and verify that there were no decreases which would have indicated loss of network PEDOT:PSS polymer. However, the dry mass was found to instead be 150% and 130% of the initial mass at day 1 for hydrogels of 40 and 80 mg mL^{-1} IL, respectively (Fig. S8, ESI†). This observed significant dry mass increase indicates the hydrogels were adsorbing components of the cell culture medium. Adsorption of media components was observed to continue over the study period of 28 days (210% and 170% of initial for 40 and 80 mg mL^{-1} hydrogels, respectively). Protein adsorption from serum is likely as others have reported protein adsorption from both defined protein solutions as well as serum-containing cell culture medium in PEDOT:PSS-containing hydrogels[45] and PEDOT:PSS thin films.[46] If assumed to protein adsorption, this is anticipated to be helpful in promoting cell attachment,[47] which was explored in greater detail in following section.

3.6. Human primary cells attach and spread on PEDOT:PSS hydrogels pre-conditioned with fetal bovine serum

Compared to conventional tissue culture plastic (TCP), hydrogels with high water content and tissue-like stiffness can better recapitulate the native microenvironment for numerous cell types. As a result, cells cultured on hydrogel substrates may serve as more representative models for understanding their innate behaviors and reactions to drugs or other stimuli.[3] Therefore, bioelectronic devices for electrical stimulation or

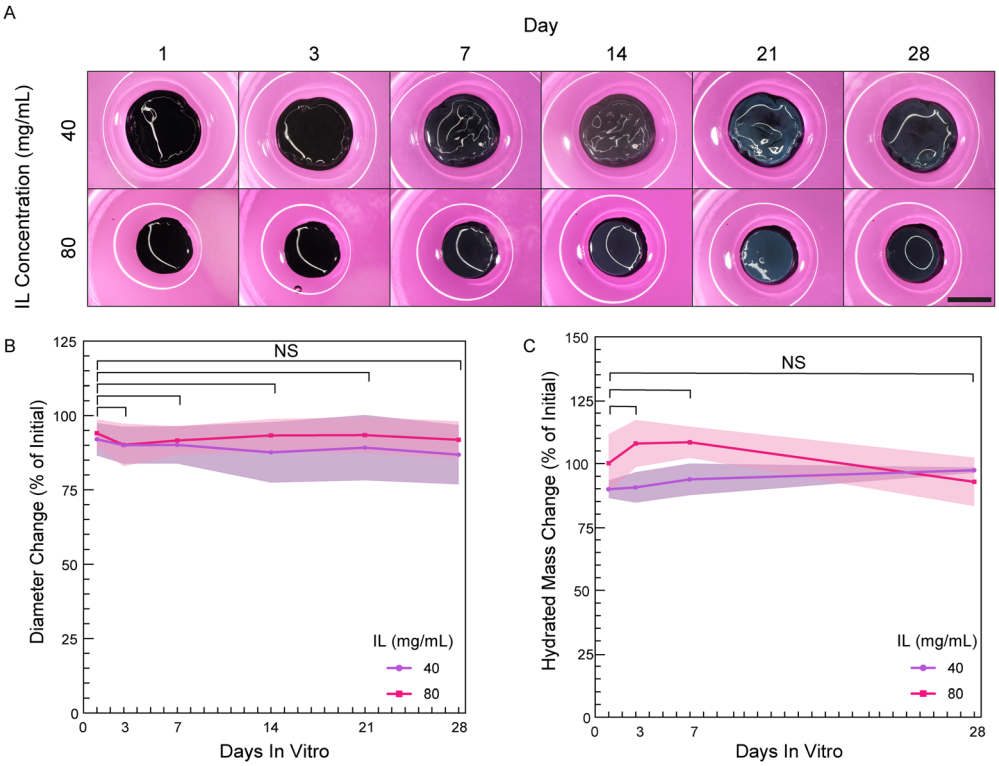

Fig. 7 PEDOT:PSS hydrogels maintain integrity in cell culture conditions for at least 28 days when cross-linked sufficiently. (A) Hydrogels fabricated with IL concentrations of 40 and 80 mg mL^{-1} qualitatively monitored for fragmentation showed no visible breakdown over 28 days. Representative images. Scale bar 5 mm. (B) and (C) Percent change in diameter and hydrated mass, respectively. No significant changes between any timepoint and day 0. Plot lines denote mean and colored shaded areas denote standard deviation. $N \geq 4$ per concentration per time point. One-way analysis of variance (ANOVA) and Dunnett's multiple comparison test with day 0 as the control. ****$P \leq 0.0001$ ***$P \leq 0.001$ **$P \leq 0.01$ *$P \leq 0.05$ non-significant (NS) $P > 0.05$.

monitoring of attached cells may result in better biointerfacing and promote tissue-relevant biology when devices are built with hydrogels rather than more traditional materials, such as metals, silicon, and plastics. While we demonstrated that these PEDOT:PSS hydrogels meet the criteria of high water fractions (>99%) and tissue-matching stiffness (1.05 to 4.13 kPa), cell attachment to these pure PEDOT:PSS hydrogel surfaces remained to be tested.

Due to its synthetic nature, it is expected that PEDOT:PSS lacks bioactive motifs that support cell adhesion. In order to facilitate cell attachment to PEDOT, various strategies have been developed including blending with extracellular matrix (ECM) protein (*e.g.* collagen)[48,49] or cell-adhesive peptides,[50] coating thin films with ECM proteins,[51,52] or soaking scaffolds in cell-type specific media.[53,54] In this study, we sought to understand if treatment with common cell culture media components changes cell attachment to pure PEDOT:PSS hydrogels, especially since the hydrogels appeared to be adsorbing media components after 1 day of incubation (Fig. S8, ESI†). To test this, hydrogels fabricated with 80 mg mL^{-1} IL were soaked in DMEM, DMEM with 10% fetal bovine serum (FBS), or 100% FBS. FBS was investigated as it is routinely used in the culture of mammalian cells, including to facilitate attachment to treated polystyrene.[55] PEDOT:PSS hydrogels were immersed in these three media prior to cell culture, which we will refer to hereafter as hydrogel pre-conditioning. For the specific cell type used here (NHDFs), it should be noted that these cells readily attach to tissue culture plastic when plated together in serum-containing media (*i.e.* TCP does not require prior plating of proteins, either as serum or a matrix coating).

After NHDF seeding and overnight culture, all conditions supported high viabilities of attached cells (98–99%; Fig. 8A and C). Despite similar viabilities, hydrogels with various pre-conditioning resulted in significant differences in cell attachment and morphology (Fig. 8A). Hydrogels pre-conditioned with 10% FBS in DMEM and 100% FBS supported the highest percent cell attachment relative to the initial plated cell density (103 ± 11.5% and 88.4 ± 14.7%, respectively), while hydrogels pre-conditioned with DMEM alone resulted in significantly lower attachment (66.9 ± 17.8%; Fig. 8B). Additionally, NHDFs on serum pre-conditioned hydrogels predominantly exhibited a more spread morphology, which is correlated with better attachment facilitated by more integrin binding to the material surface.[56] The observed spread morphology was confirmed by quantification of a larger cell area and lower circularity (Fig. 8D and Fig. S9, ESI†). In contrast, more rounded cells with smaller areas were measured on hydrogels pre-conditioned with DMEM. In conclusion, pre-conditioning PEDOT:PSS hydrogels

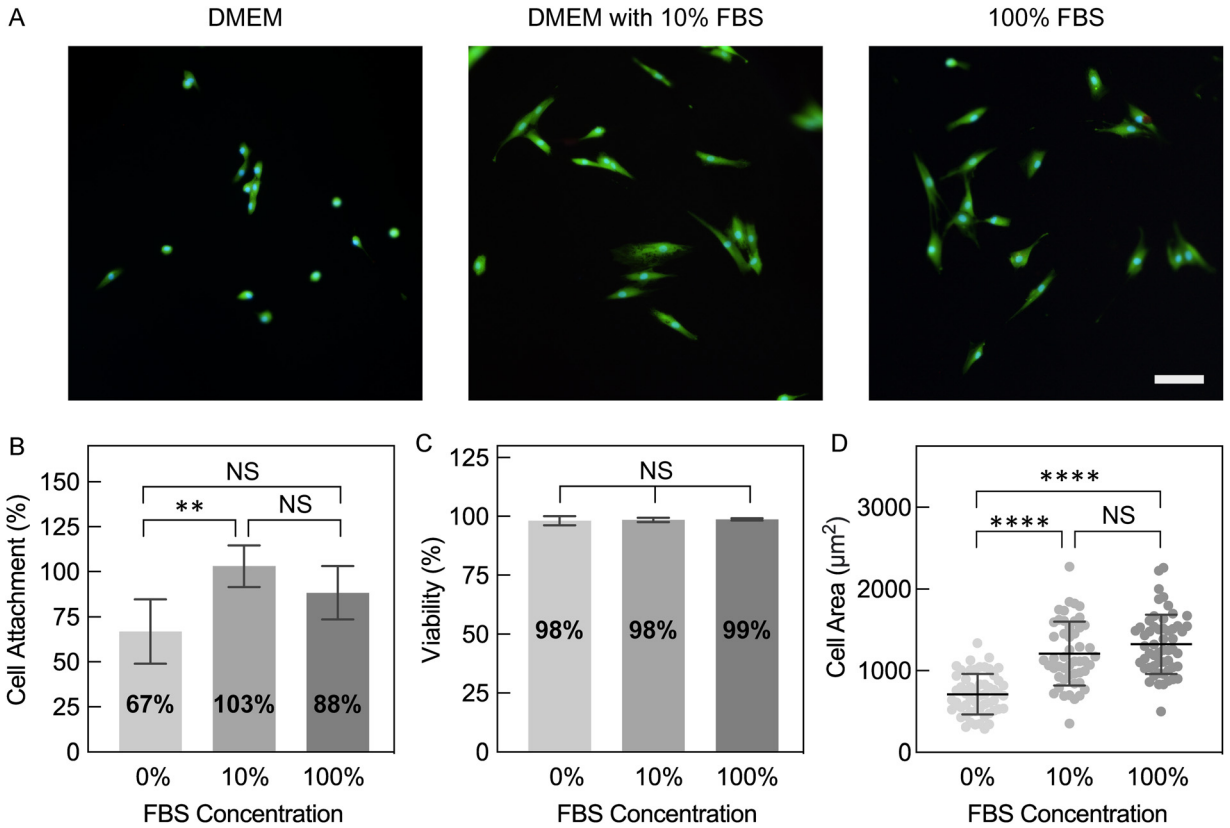

Fig. 8 Pre-conditioning hydrogels with serum-containing media enhances attachment and spreading of human fibroblasts. PEDOT:PSS hydrogels were fabricated with 80 mg mL^{-1} IL. (A) Representative epi-fluorescence images of normal human dermal fibroblasts (NHDFs) on PEDOT:PSS hydrogels pre-conditioned with Dulbecco's Modified Eagle Medium (DMEM), 10% fetal bovine serum (FBS) in DMEM and 100% FBS. Cells were stained with LIVE/DEAD™ (Calcein AM/green; ethidium homodimer-1/red) and Hoechst (blue) after overnight culture. (B) Cell density after overnight culture as percentages of initial seeded cells. Hydrogels pre-conditioned with 10% and 100% FBS had significantly higher cell attachment compared to DMEM. $N = 5$ hydrogels per condition. (C) Viability of cells. $N = 5$ hydrogels per condition. All conditions supported highly viable cells. (D) Area of attached cells ($N > 50$ cells from 5 hydrogels per condition) on hydrogels pre-conditioned with 10% and 100% FBS was significantly larger than those on gels pre-conditioned without serum. Mean and standard deviation presented. One-way analysis of variance (ANOVA) and Tukey's multiple comparison test: ****$P \leq 0.0001$ ***$P \leq 0.001$ **$P \leq 0.01$ *$P \leq 0.05$ non-significant (NS) $P > 0.05$.

in serum-containing media not only ensured successful seeding of fibroblasts, but also encouraged better attachment.

3.7. PEDOT:PSS hydrogels support viable and proliferating human primary cells over two weeks *in vitro*

To determine the cytocompatibility of PEDOT:PSS hydrogels, NHDFs were seeded and maintained for 14 days (Fig. 9A). Hydrogels fabricated with 40 and 80 mg mL^{-1} IL were tested to evaluate if different degrees of cross-linking affect seeded cells. Both hydrogel groups were pre-conditioned with 100% FBS. Throughout culture, hydrogels fabricated with 40 mg mL^{-1} IL had slightly lower cell density compared to those with 80 mg mL^{-1}, but this difference was not statistically significant (Fig. 9B). Interestingly, despite a lower seeding efficiency, cells on both hydrogel conditions exhibited a higher fold expansion compared to cells on TCP until confluent (day 7, Table S4, ESI†). Fibroblasts have been reported to undergo faster proliferation on stiffer substrates,[57,58] and thus, TCP might have been expected to result in a faster proliferation rate. Our results suggest here that the inherent properties of PEDOT:PSS hydrogels may be playing a role in the observed promotion of fibroblast expansion relative to the stiffer substrate control of TCP.

High viability of NHDFs was maintained throughout the culture period (96–99%, Fig. 9C). There was a non-significant decrease in viability from 98–99% on day 7 to 96% on day 14 for both hydrogel conditions, which is believed to be due to contact inhibition caused by over-confluence. Our results here confirm that PEDOT:PSS hydrogels fabricated with IL can support and sustain a population of NHDFs for at least two weeks. The high cytocompatibility further proves that these hydrogels are excellent candidates for biointerfacing applications. This particular hydrogel form factor of cylinders was used for 2D cell culture (cells seeded on top of a substrate) which allowed fast imaging and quantification of cells, and could be used for providing a native-like environment for cells of epithelial and endothelial lineages[3] that favor culture as cell sheets. In future work, PEDOT:PSS hydrogel with microporosity may also be fabricated to provide a 3D environment that may be suitable for other cell types.

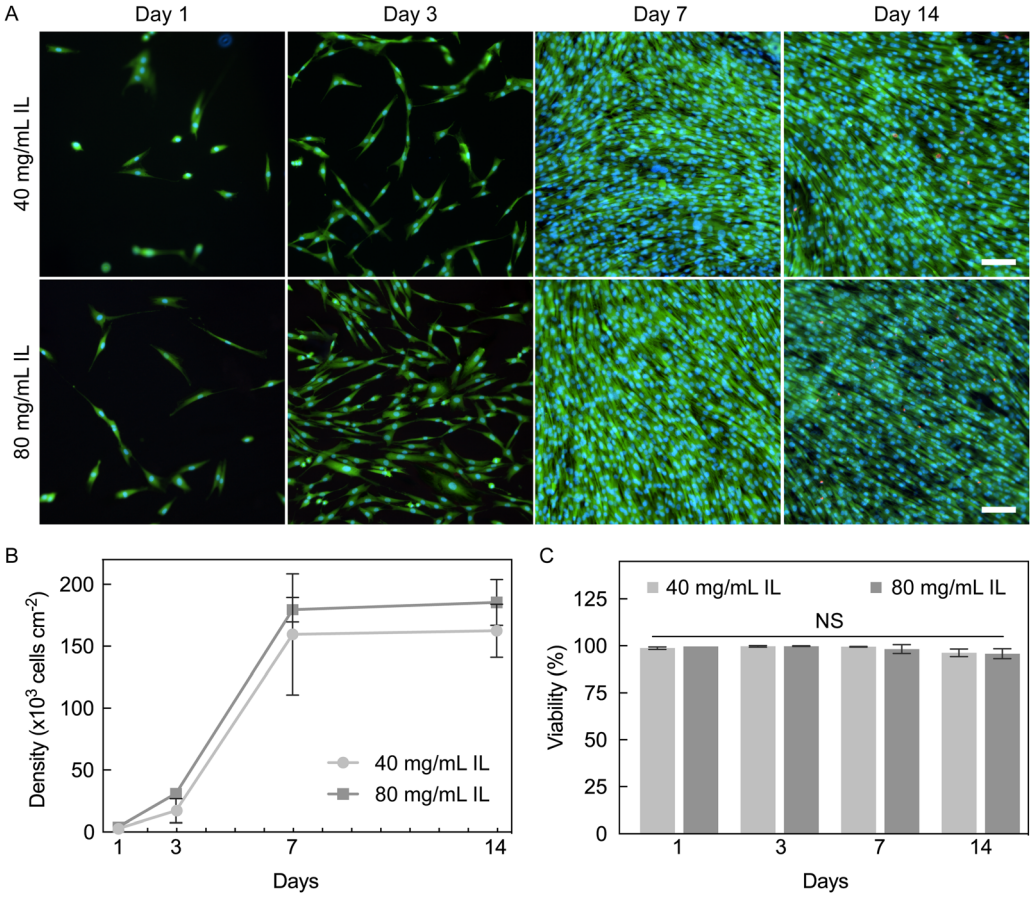

Fig. 9 PEDOT:PSS hydrogels support proliferation and viability of human fibroblasts over 14 days. Hydrogels were pre-conditioned with fetal bovine serum (FBS) (A) representative epi-fluorescence images of normal human dermal fibroblasts (NHDFs) on PEDOT:PSS hydrogels fabricated with 40 (top) or 80 mg mL^{-1} IL (bottom) over 14 days. Cells were stained with LIVE/DEAD™ (Calcein AM; green/ethidium homodimer-1; red), and Hoechst (blue). Cells were confluent at seven days and remained so thereafter. (B) Density and (C) viability of attached cells. NHDFs were highly viable and proliferated on both hydrogel conditions; no significant differences between IL concentrations were observed ($P = 0.0922$). $N = 3–4$ hydrogels per condition, 3–4 ROIs was averaged per hydrogel. Two-way analysis of variance (ANOVA) and Šidák's multiple comparison test: non-significant (NS) $P > 0.05$.

4. Conclusion

Degree of cross-linking in PEDOT:PSS hydrogels was manipulated with various ionic liquid concentrations (5–100 mg mL^{-1}). As the ionic liquid concentration increased, gelation kinetics at room temperature quickened, working time shortened, and viscosity increased. These findings have implications for solution-based processing of PEDOT:PSS-IL mixtures for hydrogel and hydrogel-based device manufacturing. The critical IL concentration needed for stability upon aqueous swelling was determined as 20 mg mL^{-1} for the specific processing utilized here (60 °C for 17.5 hours). Further verifying increased cross-linking, dimensional swelling decreased and stiffness and conductivity increased with increasing ionic liquid concentration. Hydrogels required sufficient washing with water to reach equilibrium swelling and remove non-network components. Establishing such washing protocols is important to prepare hydrogels for property measurements and biointerfacing evaluations. Final water fractions exceeded 99% confirming the heavily hydrated nature true of hydrogels. PEDOT:PSS hydrogels were stable by hydrated mass and dimensional swelling by diameter in sterile cell culture conditions for at least 28 days when cross-linked sufficiently. Additionally, PEDOT:PSS hydrogels supported a proliferating population of human primary cells (fibroblasts), which attached and exhibited normal morphology after pre-conditioning hydrogels with serum. Collectively, our results of stability and cytocompatibility illustrate these PEDOT:PSS hydrogels have significant promise for soft biointerfacing of bioelectronic devices.

Author contributions

A. P. G., T. L., S. S. O., and A. L. R. envisioned the study, contributed to experimental design and data interpretation, and wrote the manuscript. A. P. G., T. L., and S. S. O. developed the hydrogel fabrication process. A. P. G. designed and performed the studies related to PEDOT:PSS-IL mixture phase, aqueous swelling stability, and *in vitro* media stability. S. S. O. designed and performed the studies of rheology and mechanical properties. S. S. O. and T. L. designed and performed conductivity studies. T. L. designed and performed the studies

related to swelling equilibrium, cell adhesion, and cell proliferation. B. A. S. aided in the design of rheological studies as well as interpretation of the data. R. M. A., S. K. M., and L. F. aided in analysis of data procured from the swelling equilibrium and cell culture studies.

Conflicts of interest

There are no conflicts of interest to declare.

Acknowledgements

This work was supported by Washington University in St. Louis through the Center for Regenerative Medicine Seed Grant, the Women's Health Technologies Collaboration Initiation Grant, and the McDonnell Center for Cellular and Molecular Neurobiology Small Grant. This work was also supported by the Center for Engineering MechanoBiology (CEMB), an NSF Science and Technology Center, under grant agreement CMMI: 15-48571. S. S. O acknowledges support from the McDonnell International Scholars Academy. The authors acknowledge financial support from Washington University in St. Louis and the Department of Mechanical Engineering and Materials Science for assistance from staff and use of instruments. The authors would also like to thank Dianne Duncan, Director of the Washington University in St. Louis Biology Department Imaging Facility, for technical assistance regarding imaging and the Setton Lab at Washington University in St. Louis for the use of equipment.

References

1 J. Li and D. J. Mooney, *Nat. Rev. Mater.*, 2016, **1**, 16071.
2 D. Seliktar, *Science*, 2012, **336**, 1124–1128.
3 S. R. Caliari and J. A. Burdick, *Nat. Methods*, 2016, **13**, 405–414.
4 S. Correa, A. K. Grosskopf, H. Lopez Hernandez, D. Chan, A. C. Yu, L. M. Stapleton and E. A. Appel, *Chem. Rev.*, 2021, **121**, 11385–11457.
5 C. M. Tringides, N. Vachicouras, I. de Lázaro, H. Wang, A. Trouillet, B. R. Seo, A. Elosegui-Artola, F. Fallegger, Y. Shin, C. Casiraghi, K. Kostarelos, S. P. Lacour and D. J. Mooney, *Nat. Nanotechnol.*, 2021, **16**, 1019–1029.
6 H. Yuk, B. Lu and X. Zhao, *Chem. Soc. Rev.*, 2019, **48**, 1642–1667.
7 F. Fu, J. Wang, H. Zeng and J. Yu, *ACS Mater. Lett.*, 2020, **2**, 1287–1301.
8 E. Zeglio, A. L. Rutz, T. E. Winkler, G. G. Malliaras and A. Herland, *Adv. Mater.*, 2019, **31**, 1806712.
9 Y. Liu, V. R. Feig and Z. Bao, *Adv. Healthcare Mater.*, 2021, **10**, 2001916.
10 S. Inal, J. Rivnay, A.-O. Suiu, G. G. Malliaras and I. McCulloch, *Acc. Chem. Res.*, 2018, **51**, 1368–1376.
11 M. J. Donahue, A. Sanchez-Sanchez, S. Inal, J. Qu, R. M. Owens, D. Mecerreyes, G. G. Malliaras and D. C. Martin, *Mater. Sci. Eng., R*, 2020, **140**, 100546.
12 R. Gangopadhyay, B. Das and M. R. Molla, *RSC Adv.*, 2014, **4**, 43912–43920.
13 Y. Xia and J. Ouyang, *ACS Appl. Mater. Interfaces*, 2012, **4**, 4131–4140.
14 B. Yao, H. Wang, Q. Zhou, M. Wu, M. Zhang, C. Li and G. Shi, *Adv. Mater.*, 2017, **29**, 1700974.
15 S. Zhang, Y. Chen, H. Liu, Z. Wang, H. Ling, C. Wang, J. Ni, B. Çelebi-Saltik, X. Wang, X. Meng, H. Kim, A. Baidya, S. Ahadian, N. Ashammakhi, M. R. Dokmeci, J. Travas-Sejdic and A. Khademhosseini, *Adv. Mater.*, 2020, **32**, 1904752.
16 M. A. Leaf and M. Muthukumar, *Macromolecules*, 2016, **49**, 4286–4294.
17 V. R. Feig, H. Tran, M. Lee and Z. Bao, *Nat. Commun.*, 2018, **9**, 2740.
18 M. Y. Teo, N. RaviChandran, N. Kim, S. Kee, L. Stuart, K. C. Aw and J. Stringer, *ACS Appl. Mater. Interfaces*, 2019, **11**, 37069–37076.
19 V. R. Feig, S. Santhanam, K. W. McConnell, K. Liu, M. Azadian, L. G. Brunel, Z. Huang, H. Tran, P. M. George and Z. Bao, *Adv. Mater. Technol.*, 2021, **6**, 2100162.
20 B. Lu, H. Yuk, S. Lin, N. Jian, K. Qu, J. Xu and X. Zhao, *Nat. Commun.*, 2019, **10**, 1043.
21 Y. Liu, J. Liu, S. Chen, T. Lei, Y. Kim, S. Niu, H. Wang, X. Wang, A. M. Foudeh, J. B.-H. Tok and Z. Bao, *Nat. Biomed. Eng.*, 2019, **3**, 58–68.
22 D. Won, J. Kim, J. Choi, H. Kim, S. Han, I. Ha, J. Bang, K. K. Kim, Y. Lee, T.-S. Kim, J.-H. Park, C.-Y. Kim and S. H. Ko, *Sci. Adv.*, 2022, **8**, eabo3209.
23 H. Shi, C. Liu, Q. Jiang and J. Xu, *Adv. Electron. Mater.*, 2015, **1**, 1500017.
24 Y. Wang, C. Zhu, R. Pfattner, H. Yan, L. Jin, S. Chen, F. Molina-Lopez, F. Lissel, J. Liu, N. I. Rabiah, Z. Chen, J. W. Chung, C. Linder, M. F. Toney, B. Murmann and Z. Bao, *Sci. Adv.*, 2017, **3**, e1602076.
25 J. Ouyang, *Displays*, 2013, **34**, 423–436.
26 T. Canal and N. A. Peppas, *J. Biomed. Mater. Res.*, 1989, **23**, 1183–1193.
27 G. D. Nicodemus and S. J. Bryant, *Tissue Eng., Part B*, 2008, **14**, 149–165.
28 X. Li, P. Zhang, Q. Li, H. Wang and C. Yang, *iScience*, 2021, **24**, 102319.
29 Z. Zhou, L. Ruiz Cantu, X. Chen, M. R. Alexander, C. J. Roberts, R. Hague, C. Tuck, D. Irvine and R. Wildman, *Addit. Manuf.*, 2019, **29**, 100792.
30 A. R. Hibbins, P. Kumar, Y. E. Choonara, P. P. D. Kondiah, T. Marimuthu, L. C. Du Toit and V. Pillay, *Polymers*, 2017, **9**, 474.
31 S. Ebnesajjad and A. H. Landrock, in *Adhesives Technology Handbook (Third Edition)*, ed. S. Ebnesajjad and A. H. Landrock, William Andrew Publishing, Boston, 2015, pp. 206–234.
32 J. Wang, Q. Li, K. Li, X. Sun, Y. Wang, T. Zhuang, J. Yan and H. Wang, *Adv. Mater.*, 2022, **34**, 2109904.

33 S. Zhang, P. Kumar, A. S. Nouas, L. Fontaine, H. Tang and F. Cicoira, *APL Mater.*, 2015, **3**, 014911.
34 J. Rivnay, H. Wang, L. Fenno, K. Deisseroth and G. G. Malliaras, *Sci. Adv.*, 2017, **3**, e1601649.
35 C. F. Guimarães, L. Gasperini, A. P. Marques and R. L. Reis, *Nat. Rev. Mater.*, 2020, **5**, 351–370.
36 J. Yang, L. Chang, C. Ma, Z. Cao and H. Liu, *Macromol. Rapid Commun.*, 2022, **43**, 2100557.
37 G. Sandu, B. Ernould, J. Rolland, N. Cheminet, J. Brassinne, P. R. Das, Y. Filinchuk, L. Cheng, L. Komsiyska, P. Dubois, S. Melinte, J.-F. Gohy, R. Lazzaroni and A. Vlad, *ACS Appl. Mater. Interfaces*, 2017, **9**, 34865–34874.
38 G. Li, K. Huang, J. Deng, M. Guo, M. Cai, Y. Zhang and C. F. Guo, *Adv. Mater.*, 2022, **34**, 2200261.
39 T. Zhou, H. Yuk, F. Hu, J. Wu, F. Tian, H. Roh, Z. Shen, G. Gu, J. Xu, B. Lu and X. Zhao, *Nat. Mater.*, 2023, **22**, 895–902.
40 H. Yuk, B. Lu, S. Lin, K. Qu, J. Xu, J. Luo and X. Zhao, *Nat. Commun.*, 2020, **11**, 1604.
41 D. M. DeLongchamp, B. D. Vogt, C. M. Brooks, K. Kano, J. Obrzut, C. A. Richter, O. A. Kirillov and E. K. Lin, *Langmuir*, 2005, **21**, 11480–11483.
42 Y. Liu, J. Liu, S. Chen, T. Lei, Y. Kim, S. Niu, H. Wang, X. Wang, A. M. Foudeh, J. B.-H. Tok and Z. Bao, *Nat. Biomed. Eng.*, 2019, **3**, 58–68.
43 V. L. Thai, D. H. Ramos-Rodriguez, M. Mesfin and J. K. Leach, *Mater. Today Bio*, 2023, **22**, 100769.
44 J. Kurowiak, A. Kaczmarek-Pawelska, A. G. Mackiewicz and R. Bedzinski, *Processes*, 2020, **8**, 304.
45 A. Casella, A. Panitch and J. K. Leach, *J. Biomed. Mater. Res., Part A*, 2023, **111**, 596–608.
46 V. Karagkiozaki, P. G. Karagiannidis, M. Gioti, P. Kavatzikidou, D. Georgiou, E. Georgaraki and S. Logothetidis, *Biochim. Biophys. Acta*, 2013, **1830**, 4294–4304.
47 Y. Yamada, G. Fichman and J. P. Schneider, *ACS Appl. Mater. Interfaces*, 2021, **13**, 8006–8014.
48 F. Furlani, M. Montanari, N. Sangiorgi, E. Saracino, E. Campodoni, A. Sanson, V. Benfenati, A. Tampieri, S. Panseri and M. Sandri, *Biomater. Sci.*, 2022, **10**, 2040–2053.
49 S. Inal, A. Hama, M. Ferro, C. Pitsalidis, J. Oziat, D. Iandolo, A.-M. Pappa, M. Hadida, M. Huerta, D. Marchat, P. Mailley and R. M. Owens, *Adv. Biosyst.*, 2017, **1**, 1700052.
50 Y. Xu, X. Yang, A. K. Thomas, P. A. Patsis, T. Kurth, M. Kräter, K. Eckert, M. Bornhäuser and Y. Zhang, *ACS Appl. Mater. Interfaces*, 2018, **10**, 14418–14425.
51 E. Šafaříková, L. Švihálková Šindlerová, S. Stříteský, L. Kubala, M. Vala, M. Weiter and J. Víteček, *Sens. Actuators, B*, 2018, **260**, 418–425.
52 S. Stříteský, A. Marková, J. Víteček, E. Šafaříková, M. Hrabal, L. Kubáč, L. Kubala, M. Weiter and M. Vala, *J. Biomed. Mater. Res., Part A*, 2018, **106**, 1121–1128.
53 I. del Agua, S. Marina, C. Pitsalidis, D. Mantione, M. Ferro, D. Iandolo, A. Sanchez-Sanchez, G. G. Malliaras, R. M. Owens and D. Mecerreyes, *ACS Omega*, 2018, **3**, 7424–7431.
54 A. K. Jayaram, C. Pitsalidis, E. Tan, C.-M. Moysidou, M. F. L. De Volder, J.-S. Kim and R. M. Owens, *Front. Chem.*, 2019, **7**, 363.
55 M. Verdanova, P. Sauerova, U. Hempel and M. H. Kalbacova, *Histochem. Cell Biol.*, 2017, **148**, 273–288.
56 T. Yeung, P. C. Georges, L. A. Flanagan, B. Marg, M. Ortiz, M. Funaki, N. Zahir, W. Ming, V. Weaver and P. A. Janmey, *Cell Motil.*, 2005, **60**, 24–34.
57 H. El-Mohri, Y. Wu, S. Mohanty and G. Ghosh, *Mater. Sci. Eng., C*, 2017, **74**, 146–151.
58 E. Hadjipanayi, V. Mudera and R. A. Brown, *J. Tissue Eng. Regener. Med.*, 2009, **3**, 77–84.